Article

Potent Nematicidal Activity and New Hybrid Metabolite Production by Disruption of a Cytochrome P450 Gene Involved in the Biosynthesis of Morphological Regulatory Arthrosporols in Nematode-Trapping Fungus Arthrobotrys oligospora

Tian-Yang Song, Zi-Fei Xu, Yong-Hong Chen, Qiu-Yan Ding, Yu-Rong Sun, Yang Miao, Ke-Qin Zhang, and Xue-Mei Niu

J. Agric. Food Chem., **Just Accepted Manuscript** • Publication Date (Web): 05 May 2017

Potent Nematicidal Activity and New Hybrid Metabolite Production by Disruption of a Cytochrome P450 Gene Involved in the Biosynthesis of Morphological Regulatory Arthrosporols in Nematode-Trapping Fungus *Arthrobotrys oligospora*

Tian-Yang Song, Zi-Fei Xu, Yong-Hong Chen, Qiu-Yan Ding, Yu-Rong Sun, Yang Miao, Ke-Qin Zhang, Xue-Mei Niu*

State Key Laboratory for Conservation and Utilization of Bio-Resources & Key Laboratory for Microbial Resources of the Ministry of Education, School of Life Science, Yunnan University, Kunming, 650091, People's Republic of China

*Corresponding author (Tel: 86-871-65032538; Fax: 86-871-65034838: E-mail: xmniu@ynu.edu.cn)

ABSTRACT

A type of polyketide synthase-terpenoid synthase (PKS-TPS) hybrid metabolites including arthrosporols with significant morphological regulatory activity have been elucidated from nematode-trapping fungus *Arthrobotrys oligospora*. Previous study suggested that the gene cluster *AOL_s00215* in *A. oligospora* was involved in production of arthrosporols. Here we report that disruption of one cytochrome P450 monooxygenase gene *AOL_s00215g280* in the cluster resulted in significant phenotypic difference and much aerial hyphae. Further bioassay indicated that the mutant showed dramatic decrease in the conidial formation but developed numerous traps and killed 85% nematodes within 6 hours in contact with prey, in sharp contrast to the wildtype strain with no obvious response. Chemical investigation revealed huge accumulation of three new PKS-TPS epoxycyclohexone derivatives with different oxygenated pattern around the epoxycyclohexone moiety and absence of arthrosporols in the cultural broth of the mutant *ΔAOL_s00215g280*. These findings suggested that study on the biosynthetic pathway for morphological regulatory metabolites in nematode-trapping fungus would provide an efficient way to develop new fungal biocontrol agents.

KEYWORDS: Nematode-trapping fungus; *Arthrobotrys oligospora*; arthrosporols; biosynthesis; terpenyl epoxycyclohexone; trap formation.

INTRODUCTION

Plant associated nematodes cause insidious disease symptoms in many crops and result in significant global crop loss annually.[1,2] As natural enemies of nematodes, nematode-trapping fungi have fascinated scientists for centuries because they are a group of soil fungi that can form complex traps to capture nematodes and play important roles in controlling nematode population density in diverse natural environments.[3-5]

Arthrobotrys oligospora has been extensively studied as a model nematode-trapping fungus for characterizing and elucidating the biology and ecology of nematode-trapping fungi.[6-8] A type of polyketide synthase-terpenoid synthase (PKS-TPS) hybrid metabolites (**1**-**7**, Figure 1), including arthrosporols (**5**-**7**) with significant morphological regulatory activity, have been reported from the strains of *A. oligospora*.[9-12] Through combination of gene targeted deletion and bioinformatics from the biosynthesis of isoepoxydon (**8**),[13,14] three genes *AOL_s00215g283*, *AOL_s00215g282*, and *AOL_s00215g281*, encoding 6-methylsalicylic acid (6-MSA, **9**) synthase, P450 monooxygenase for m-cresol (**10**) and decarboxylase for 6-MSA, respectively, were characterized to play key roles in the biosynthesis for the morphological regulatory hybrid arthrosporols in *A. oligospora*.[15,16] Interestingly, disruption of the 6-MSA synthase gene led to not only the absence of arthrosporols in the mutant Δ*AOL_s00215g283*, but also the increases in the trap formation by 10 times higher than the wild-type strain.[15] What is more, two precursors, 6-MSA and m-cresol involved in the biosynthetic pathway for arthrosporols were found to display moderate nematicidal activity toward root-knot nematode *Meloidogyne incognita*.[16]

In our further study on the biosynthesis of arthrosporols, we found one gene *AOL_s00215g280* just next to the gene *AOL_s00215g281* in the upstream flanking region. Here we report the identification of the gene *AOL_s00215g280* putatively designed as a cytochrome P450 monooxygenase by gene engineering and chemical metabolite profiling.

MATERIALS AND METHODS

Sequences and phylogenetic analysis of *AOL_s00215g280* in *A. oligospora*

A web-based bioinformatics platform antiSMASH 3.0,[17] was applied to perform genome mining of the biosynthetic gene clusters. Predicted *AOL_s00215g280* in *A. oligospora* YMF1.01883 (ATCC 24927) were annotated by BLAST searches against protein databases, and by InterProScan searches against protein domain databases.[18] The conserved functional domains were analyzed using InterProScan with default parameter settings. The amino acid sequences of *AOL_s00215g280* in *A. oligospora* and the sequences from different fungi were downloaded from GenBank.[19] The amino acid sequences from different fungi were analyzed using the DNAman software package, ver. 5.2.2, (Lynnon BLLC, San Ramon, CA). Two neighbor-joining trees were constructed using the Mega 5.1 software package.

Construction of disruption vector

A. oligospora YMF 1.3170 strain used as the wild strain in this study was described in our previous study.[15] Genomic DNA of *A. oligospora* YMF 1.3170 was extracted as previously described.[6] Restriction endonucleases and DNA modifying enzymes were purchased from New England Biolabs (Beverly, MA). In-Fusion® HD Cloning Kits were purchased from Clontech Laboratories (Mountain View, CA). The left and right DNA fragments flanking the hygromycin resistant gene (hygR) in pAg1-H3 vector were amplified from the genomic DNA of *A. oligospora* YMF 1.3170 by PCR (GXL high-fidelity DNA Polymerase TaKaRa Biotechnology Co. Ltd, Dalian, China) using primer sets as described in Table 1.

The DNA fragments (5' flank 2064-bp and 3' flank 1812-bp) were purified using PCR Clean-up Kit (Macherey-Nagel Inc, Düren, Germany) and NucleoSpin Gel, and were inserted into the specific sites of pAg1-H3 vector (Table 1), respectively, by In-Fusion method to generate the pAg1-H3-5′-3′ vector. The homologous fragment amplifications were carried out as follows. Twenty-five μL PCR amplification system with using GXL high-fidelity DNA polymerase following the manufacturer's instructions (Takara) was applied. Half of one microliter of the prepared genomic DNA from *A. oligospora* YMF 1.3170 was added as template. All PCRs were performed in a Veriti 96-well thermal cycler (Applied

Biosystems, Foster city, CA). The amplification program contained predenaturation at 98 °C for 4 min followed by 30 cycles of denaturation at 98 °C for 10 s, annealing at 57 °C for 15 s, and elongation at 68 °C for 2 min, with a final extension step at 68 °C for 10 min.

Preparation of fungal protoplasts

Medium PDASS (PDA supplemented with 0.6 M sucrose, 0.3 g/L yeast extract, 0.3 g/L tryptone, 0.3 g/L peptone, and 200 μg/mL hygromycin B (Roche Applied Science, Mannheim, Germany) for selecting transformants) was applied to carry out protoplast regeneration. Four 1-1.2 cm diameter mycelia plugs from 7-day old fungal strain on YMA medium (2 g/L yeast extract, 10 g/L malt extract, and 18 g/L agar) at 28 °C were inoculated into 100 mL of TG medium [1% tryptone (Oxoid, Basingstoke, U.K.), and 1% glucose] and cultured at 30 °C at 180 rpm for 36 h. The mycelia were harvested and resuspended in 20 mL of a filter-sterilized enzyme solution that contained 120 mg of lysing enzymes (Sigma, St. Louis, MO), 0.4 mL of cellulase (Sigma, St. Louis, MO), and 100 mg of snailase (Solarbio, Beijing, China) in 0.6 M $MgSO_4$ at pH 6.0. The suspension was incubated for 4 h at 28 °C on a rotary shaker at 180 rpm. Protoplasts were collected by filtering through six layers of sterile lens-cleaning tissue and centrifuged at 1000 g. The protoplasts were washed twice with KTC (1.2 M KCl, 10 mM Tris-HCl, 50 mM $CaCl_2$) solution and finally resuspended in the same solution.

Transformation of fungus *A. oligospora*

The protoplast-based protocol for the disruption of the P450 gene *AOL_s00215g280* in *A. oligospora* YMF 1.3170 was performed as described previously.[15,16] About 150 μL protoplasts (circa 8.0×10^7 /mL) were mixed with 10 μg linear DNA in a 1.5 mL centrifuge tube. After 30 min of incubation on ice, 600 μL of PTC (50 mM $CaCl_2$, 20 mM Tris-HCl, 50% polyethylene glycol 6000, pH 7.5) was added into the mixture and mixed gently. After incubation at 28 °C for 1 h, regeneration for 12 h, the putatively transformed protoplasts were plated onto PDAS medium (PDA supplemented with 5 g/L molasses, 0.6 M saccharose, 0.3 g/L yeast extract, 0.3 g/L tryptone, and 0.3 g/L casein peptone) containing 200 μg/mL

of hygromycin B. Transformation colonies were selected after incubation at 28 °C for 6-8 d, and every single colony was transferred to a new plate containing TYGA medium (10 g/L tryptone, 10 g/L glucose, 5 g/L yeast extract, 5 g/L molasses, 18 g/L agar) containing 200 μg/mL of hygromycin B. After incubation for 5 d at 28 °C, genomic DNA of putative transformants were extracted and were verified by PCR to check for the integration of genes in the genome.

Vegetative growth and conidia yield comparisons

About 6 mm diameter mycelia plugs from 7 d fungal colonies of the wildtype and the mutant strains were inoculated onto 9 cm plates with different media (5 replicates per strain), respectively, and then incubated at 28 °C for 4–8 d. Radial colony growth rates and colony morphology were analyzed at 24 h interval for 10 d and growth rate calculated as mm/h each day. The growth rates and the colony morphology of the wildtype and the mutant strains were compared on PDA, TYGA, and YMA (2 g/L yeast extract, 10 g/L malt extract, and 18 g/L agar) respectively.

To assess sporulation capacities of the wildtype and the mutant strains, 100 μL aliquots of 10^6 conidial suspension were spread on 9 cm plates with YMA medium and incubated for 10 d at 28 °C, the conidia were washed into 10 mL sterile water, followed by filtration through four layers of len tissues to remove mycelia debris. The concentrations of the conidial suspension were determined with microscopic counts on a haemocytometer.[20]

Induction of trap formation and virulence assays

Both the wildtype and the mutant strains were cultivated on agar plates by spreading approximately 10^6 conidia per plate. After 3 d of incubation at 28 °C, about 400 adult *Caenorhabditis elegans* (strain N2) nematodes were added into the middle of the plate. Live specimens of the model nematode *C. elegan* N2 strains were propagated at 20 °C with 42% relative humidity in the dark on nematode growth medium (NGM) plates using *Escherichia coli* strain OP50 as a food source for 4-6 d in advance. Fungal

morphological traits including trap formation were observed and the numbers of captured nematodes were recorded after 12 and 24 h, respectively, under light microscopy. The experiments were performed in triplicate.

Fermentation and extraction procedures.

The wildtype *A. oligospora* and the mutant Δ*AOL_s00215g280* strain cultured on PDA medium at 28 °C for 10 d were inoculated into 500 mL flasks containing 200 mL of production PD medium (potato 200 g/L and dextrose 20 g/L), respectively. The culture broths of the 10 d liquid fermentations (1.5 L each strain) were filtered to separate the mycelia from the cultures. The culture filtrates were concentrated *in vacuo* to 50 mL and were extracted overnight with ethyl acetate (1:1 v/v). The organic fractions were evaporated to dryness to give residues. The dried organic residues were then dissolved in 500 μL of methanol, filtered through 0.22 μm membranes, and further analyzed using HPLC-DAD.

HPLC analysis

HPLC analysis was carried out on a CAPCELL PAK C18 column (5 μm; 4.6 × 250 mm, Shiseido, Tokyo, Japan) by using a HP 1200 unit (Agilent, Waldbronn, Germany). The instrumental conditions were as followed: mobile phase A was 0.1% formic acid in water and mobile phase B was 0.1% formic acid in acetonitrile and the total flow rate was 1 mL/min; column temperature was maintained at 40 °C; injection volume for the extracts was 25 μL. The LC conditions were manually optimized based on separation patterns and were as follows: gradient program of B (0 min 10% B; 2 min 10% B; 10 min 25% B; 30 min 35% B; 35 min 50% B; 45 min 90% B; 47 min 10% B; 49 min 10% B). UV spectra were recorded at 220 to 400 nm. The standard sample arthrosporol A (**4**) was isolated from wildtype *A. oligospora* according to the modified method described in the literature.[21]

Purification and identification of the intermediates from the mutant strain

The 14 d cultural broth of the mutant Δ*AOL_s00215g280* cultured on 20L PD liquid medium were concentrated *in vacuo* and partitioned with acetyl acetate. The acetyl acetate part was evaporated to dryness to give residue. The residue was dissolved in methanol and filtered with through 0.22 μm membranes. The filtrate was loaded onto a CAPCELL PAK C18 column (5 μm; 4.6 × 250 mm, Shiseido) eluting with H_2O−MeOH (10−90%) with decreasing polarity through a continuous gradient. The purified samples were structurally elucidated with NMR data.

$C_{280\text{-}1}$ (11): $C_{14}H_{18}O_5$; Colorless oil; $[\alpha]_D^{21.9}$ -83.33 ° (*c* 0.18, MeOH); UV (MeOH) λmax (log *ε*) 203.0 (4.24), 219.0 (4.13) nm; IR (KBr) ν_{max} 3423, 3035, 2958, 2925, 2856, 2731, 1675, 1579, 1439, 1384, 1311, 1262, 1215, 1195, 1168, 1101, 1046, 1027, 948, 882, 862, 805, 738, 707, 650, 617, 596, 566, 546 cm^{-1}; ^1H NMR and ^{13}C NMR, see Table 2; Positive HRESI-MS *m*/*z*: 289.1029 $[M+Na]^+$; Negative HRESI-MS *m*/*z*: 265.1021 $[M-H]^-$, calculated as 265.1028 for $C_{14}H_{17}O_5$.

$C_{280\text{-}2}$ (12): $C_{17}H_{22}O_5$; Colorless oil; $[\alpha]_D^{22.0}$ -198.33 ° (*c* 0.20, MeOH); UV (MeOH) λmax (log *ε*) 207.0 (4.86), 220.0 (4.79) nm; IR (KBr) ν_{max} 3422, 3031, 2926, 2856, 1677, 1569, 1435, 1403, 1383, 1307, 1263, 1206, 1099, 1041, 1028, 884, 863, 802, 742, 617, 583, 561, 414 cm^{-1}; ^1H NMR and ^{13}C NMR, see Table 2; Positive HRESI-MS *m*/*z*: 329.1437 $[M+Na]^+$; Negative HRESI-MS *m*/*z*: 305.1337 $[M-H]^-$, calculated as 305.1332 for $C_{17}H_{21}O_5$.

$C_{280\text{-}3}$ (13): $C_{17}H_{24}O_5$; $[\alpha]_D^{22.0}$ -132.29 (*c* = 0.16, MeOH); UV (MeOH) λ_{max} (log *ε*): 204.5 (3.83), 219 (3.80) nm; IR (KBr) ν_{max}: 3413, 3038, 2974, 2935, 2861, 2733, 2652, 1707, 1677, 1562, 1552, 1501, 1462, 1441, 1384, 1307, 1223, 1185, 1168, 1124.46, 1104, 1045, 1024, 968, 922, 906, 868, 799, 739, 712, 648, 620 577, 532, 506, 472, 408 cm^{-1}; ^1H NMR and ^{13}C NMR, see Table 2; Positive HRESI-MS *m*/*z*: 331.1512 $[M+Na]^+$; Negative HRESI-MS *m*/*z*: 307.1544 $[M-H]^-$, calculated as 307.1514 for $C_{17}H_{23}O_5$.

Optical rotations were measured on a Horiba-SEAP-300 spectropolarimeter. UV spectroscopic data were recorded on a Shimadzu-210A double-beam spectrophotometer. IR spectra of samples in KBr disks were recorded on a Bruker-Tensor-27 spectrometer with KBr pellets. NMR spectra were obtained

on a Bruker DRX-500 spectrometer with respect to solvent as internal standard. MS were carried out on a VG-Auto-Spec-3000 spectrometer.

Statistical analysis

Statistical analysis were performed using the SPSS package, version 17.0 for Windows (SPSS Inc., Chicago, IL). Differences with $P < 0.05$ were regarded as statistically significant, $P < 0.01$ as highly statistically significant.

RESULTS AND DISCUSSION

Bioinformatics analysis suggested that the gene *AOL_s00215g280* was annotated for a cytochrome P450 monooxygenase. Twenty-one homologs of AOL_s00215g280 were retrieved and one neighbor-joining phylogenetic tree was built using the amino acid sequences of these proteins (Figure 2). AOL_s00215g280 was clustered within the fungal cytochrome P450 monooxygenases, and formed a distinct monophyletic branch with no other closely related homologs as of yet. Like AOL_s00215g283 AOL_s00215g282 and AOL_s00215g281,[6,15,16] no homologs from other nematode-trapping fungi such as *Dactylellina haptotyla* and *Drechslerella stenobrocha* were found to cluster with the amino acid sequences of *AOL_s00215g280*.

Further analysis revealed that the amino acid sequence of AOL_s00215g280 shares 59% similarity to cytochrome P450 yanH that has been assumed to hydroxylate the methyl at C-2 of the PKS-derived epoxycyclohexenol moiety of 7-deacetoxyyanuthone A to 22-deacetoxyyanuthone A.[22] To elucidate the function of the gene *AOL_s00215g280* involved in the biosynthesis of arthrosporols, we first constructed the mutant with knockout of the gene *AOL_s00215g280* by genetic manipulation. A protoplast transformation method for genetic disruption of targeted gene in *A. oligospora* was developed using double-crossover recombination with the hygromycin-resistance gene (hyg) as a selection marker (Figure 3A-3B). The mutant Δ*AOL_s00215g280* was screened from 23 transformants by genomic

DNAs isolation and diagnostic PCR (Figure 3C). Compared to a 1317-bp fragment from the wildtype strain of *A. oligospora*, a 2976-bp fragment was amplified from the mutant short of the gene *AOL_s00215g280* using the primers 280yz-5f/280yz-3r (Figure 3C and Table 1).

Morphological analysis was performed on three media PDA, TYGA, and YMA. Compared to the wildtype strain, the mutant Δ*AOL_s00215g280* showed significantly decreased growth rates from day 2 to day 8 (Figure 4) and exhibited different mycelial morphology. After 5 d, the mutant developed much more fluffy aerial hypha than the wildtype strain (Figure 4). It was obvious that the deletion of the gene *AOL_s00215g280* could lead to the altered growth rate and quite different phenotype of the nematode-trapping fungus. In addition, the deletion of the gene *AOL_s00215g280* caused significant decrease in the spore formation and germination (Figures 5A and 5B). It was interesting to note that the mutant Δ*AOL_s00215g280* formed far more adhesive networks in a shorter time than the wildtype strain after the nematodes *C. elegans* were added on the 3 d cultures (Figure 5C). Within 6h, the numbers of the adhesive traps formed by the mutant were about 385/cm^2 (Figure 5C), while the wild type strain did not develop any traps. At the same time, the traps formed by the mutant Δ*AOL_s00215g280* captured almost 85% of the tested nematodes (Figure 5D). At 24h, all the nematodes in the mutant group showed much more deformed and degraded shapes than those in the wildtype group (Figure 5), indicative of the amazing powerful nematicidal activity of the mutant.

HPLC method was applied to analyze the chemical metabolite profiles of the methanolic extracts of the mutant Δ*AOL_s00215g280* strain and the wildtype strain (Figure 6). Compared to the wildtype strain, the mutant Δ*AOL_s00215g280* strain displayed a predominant peak at 19-20 min, and three distinct peaks at around 11, 34 and 35 min in the HPLC profile. (Figure 6). Further detailed analysis showed that no arthrosporol A was detected in the cultural broth of the mutant Δ*AOL_s00215g280* (Figure 6), indicating that the disruption of the gene *AOL_s00215g280* led to loss of arthrosporol A and the gene *AOL_s00215g280* was involved in the biosynthetic pathway for arthrosporol A. Among these distinct peaks in the metabolic profile of the mutant Δ*AOL_s00215g280*, three peaks at around 19, 34 and 35

min, showed quite similar UV absorptions at 207 and 220 nm. Thus, the mutant strain Δ*AOL_s00215g280* was cultivated on a larger scale of 20 L. Chemical investigation on the crude extract of this cultural broth of the mutant Δ*AOL_s00215g280* led to successful isolation of the above targeted metabolites. Their structures were fully determined by MS, 1D and 2D NMR data.

Metabolite **$C_{280\text{-}1}$** (**11**) was isolated as a colorless oil. It exhibited quasimolecular ion peaks at *m/z* 289.1029 $[M+Na]^+$ and 265.1021 $[M-H]^-$ in the positive and negative HRESI-MS, respectively, and was assigned to a molecular formula of $C_{14}H_{18}O_5$. The ^{1}H NMR spectrum of **11** (Table 2) displayed two methyls attached to double bonds at δ_H 1.56 and 1.91 (each 3H, s), two oxygenated methine protons at δ_H 4.24 (1H, s) and 3.53 (1H, s), and two olefinic protons at δ_H 5.68 (1H, s), and 5.24 (1H, t, J = 5.5 Hz). Other protons at δ_H 2.03-2.10 and 2.90 were also observed in the ^{1}H NMR spectrum of **11**. The ^{13}C NMR spectroscopic data of **11** demonstrated only 13 carbon resonances. These carbon signals were further classified by DEPT-90 and DEPT-135 experiments as two olefinic methyls (δ_C 21.2 and 16.3), three methylenes (δ_C 28.3, 35.5 and 34.7), two oxymethines (δ_C 67.4 and 63.9), one oxygenated quaternary carbon (δ_C 60.2), two olefinic methines (δ_C 124.7 and 118.5), two olefinic quaternary carbons (δ_C 158.0 and 138.8) and a keto carbon (δ_C 195.6). The 1D NMR data of **11** indicated the characteristic signals for an epoxy ring and an α,β-unsaturated ketone system, similar to those in known oligosporon (**1**).[9,10] Detailed comparison revealed that **11** had a similar epoxy-cyclohexenol moiety to **1**, except for the ketone positioned at C-4 in the epoxy-cyclohexenol moiety of **11** instead of at C-1, due to the dramatically downfield shift of C-2 from δ_C 142 in **1** to 158 ppm in **11**. This was also confirmed by the significant ^{1}H–^{13}C long-range correlation of the H_2-1′at δ_H 2.10 with the ketone at δ_C 195.6 in the HMBC spectrum of **11** (Figure 7). The significant ^{1}H-^{13}C long-range correlations of a carbon at δ_C 177.2 with the olefinic methine proton δ_H 5.24 and the methylene protons at δ_H 2.90 suggested the presence of one extra carboxyl group in **11**, whose chemical signal was not appearing in the ^{13}C NMR spectrum of **11**. Together with the ^{1}H-^{1}H COSY correlations of the olefinic methine proton at δ_H 5.24 and the methylene protons at δ_H 2.90 and one methyl protons at δ_H 1.56 (Figure 7), one segment of the structure

11, $COOHCH_2CH=C(CH_3)$- was established. The methyl protons at δ_H 1.56 further showed the HMBC correlations with the quaternary carbon at δ_C 138.8 and one methylene carbon at δ_C 35.5, and the latter methylene protons displayed the HMBC correlations with another methylene carbon at δ_C 28.3 and the oxygenated quaternary carbon at δ_C 60.2, indicating a side chain $COOHCH_2CH=C(CH_3)$-CH_2CH_2- attached to the epoxy-cyclohexenol moiety as described in Figure 7. The NOE correlations of H-4'/H_2-2' and H_2-5'/3'-CH_3 indicated the *E* configuration of the double bond between C-3' and C-4'. The stereochemistry of the epoxy-ring and C-1 in the cyclohexendiol moiety was determined to be the same as those of known metabolites (**3**-**7**), according to their similar biogenesis and corresponding NOE correlations (Figure 7).

Metabolite $\mathbf{C_{280\text{-}2}}$ (**12**) exhibited quasimolecular ion peaks at *m/z* 331.1512 $[M+Na]^+$ and 307.1544 $[M-H]^-$ in the positive and negative HRESI-MS, respectively, and was assigned to a molecular formula of $C_{17}H_{24}O_5$. The ^1H, ^{13}C NMR and DEPT spectra (Table 2) of **12** displayed that compound **12** closely resembled **11**. Comparison of the NMR data of **12** with those of **11** revealed that they shared the same epoxy-cyclohexenol moiety and the carboxyl group. The differences between them came from the side chains. Interpretation of the $^1H-^1H$ COSY spectrum of **12** led to unambiguous establishment of two segments, the moieties 7′-CH_3/H-7′, and 3′-CH_3/H-2′/H_2-1′ (Figure 7). The $^1H-^{13}C$ correlations of 7′-CH_3 at δ_H 1.63 with one methylene carbon at δ_C 34.1 (C6') and one methine carbon at δ_C 39.8 (C7'), and the carboxyl carbon at δ_C 177.9 (C8'), of 7-H' at δ_H 2.42 with two methylene carbons C5' (δ_C 26.3), C6' and C8', and of 4-H' at δ_H 2.00 with C5', C6', C-2' (δ_C 118.4) and 3′-CH_3 (δ_C 17.7), led to elucidation of a side chain $COOH(CH_3)CHCH_2CH_2CH_2$-$(CH_3)C=CHCH_2$- attached to the epoxy-cyclohexenol moiety in **12** (Figure 7). The NOE correlations of H-2'/H-4' and H-1'/3′-CH_3 in the ROESY spectrum of **12** suggested the double bond between C-2' and C-3' as *E* configuration in **12**.

Metabolite $\mathbf{C_{280\text{-}3}}$ (**13**) was isolated as a colorless oil. It exhibited quasimolecular ion peaks at *m/z* 329.1437 $[M+Na]^+$ and 305.1337 $[M-H]^-$ in the positive and negative HRESI-MS, respectively, and was assigned to a molecular formula of $C_{17}H_{22}O_5$. Comparison of the NMR spectroscopic data of **13** with those of **12** suggested that they were quite similar except that **13** possessed the double bond between C-

6′ and C-7′ due to the significant highfield shift of the carboxyl carbon value from δ_C 177.9 in **12** to δ_C 169.5 in **13**, which was confirmed by 2D NMR spectroscopic data. The ROESY correlation of H_2-5′ and 7′-CH_3 in the NOESY spectrum of **13** indicated the configuration of the double bond between C-6′ and C-7′ as *E*. The structure of **13** was finally elucidated as 6′,7′-didehydro derivative of **12.**

Thus, metabolites **11**-**13** were fully determined as three new derivatives of PKS-TPS hybrid epoxy-cyclohexenoids. From a structural point of view, they might derive from an intermediate farnesyl epoxy-cyclohexenone (**14**) via oxidative cleavages in the farnesyl chain, as seen in yanuthones from marine isolates *Aspergillus niger*.[23-25] It was remarkable to note that all the known PKS-TPS hybrid metabolites previously reported from nematode-trapping fungus *A. oligospora* up to date, only had two oxygenated patterns around the epoxy cores including 1: ketone at C-1 and hydroxyl at C-4 as in oligosporons (**1-2**), and 2: both hydroxyls at C-1 and C-4 as in arthrobotrisins (**3-4**)[11] and arthrosporols (**5-7**)[12] (Figure 1). This is for the first time that the PKS-TPS hybrid metabolites with ketone at C-4 and hydroxyl at C-1 from *A. oligospora* were reported.

These three metabolites were evaluated for their inhibitory activities toward nematode *C. elegans* (Figure 8). It is interesting to note that within 6 h, these three metabolites at concentrations of ≥50 μg/mL showed stronger inhibitory activity toward nematodes than positive control avermectins. Within 6 h, metabolite **11** inhibited about 30% nematodes and metabolites **12** and **13** suppressed about 20%, while avermectins inhibited showed less than 5% inhibitory activity. However, the inhibitory effects of these metabolites **11**-**13** did not increase with time as did avermectins. This could be partly ascribed to the fact that all metabolites of this PKS-TPS hybrid group from *A. oligospora* were rather unstable, decomposing on storage even when refrigerated.[9,10]

In conclusion, by gene engineering and chemical metabolite profiling, we showed that the disruption of the P450 gene *AOL_s00215g280* avoided the production of arthrosporol metabolites in the mutant and led to significant decrease in conidial development and dramatic increase in trap formation. The mutant short of the P450 gene *AOL_s00215g280* demonstrated powerful nematicidal activity with killing 85% nematodes within 6 h. A class of three new derivatives of terpenyl epoxy-cyclohexenoids were also

obtained. These results suggest that the P450 gene *AOL_s00215g280* was not only involved in the biosynthesis for arthrosporols, but also attributed to the regulation in trap formation and fungal predatory ability.

ACKNOWLEDGMENT

This work was sponsored by projects from 973 Program on Biological Control of Key Crop Pathogenic Nematodes (2013CB127505), National Natural Science Foundation of China (U1502262 and 31470169), and Yunnan University Program for Excellent Young Talents awarded to X.N. (XT412003).

SUPPORTING INFORMATION

Spectroscopic data (1D and 2D NMR spectra) of compounds **11**−**13**. This information is available free of charge via the Internet at http://pubs.acs.org.

REFERENCES

(1) Nicol, J. M.; Turner, S. J.; Coyne, D. L.; den Nijs, L.; Hockland, S.; Tahna Maafi, Z. Current nematode threats to world agriculture. In *Genomics and Molecular Genetics of Plant Nematode Interactions*; Jones, J., Gheysen, G., Fenoll, C., Eds.; Springer: Dordrecht, Netherlands, **2011**; pp. 21–43.

(2) Castagnone-Sereno, P.; Danchin, E. G.; Perfus-Barbeoch, L.; Abad, P. Diversity and evolution of root-knot nematodes, genus *Meloidogyne*: new insights from the genomic era. *Annu. Rev. Phytopathol*. **2013**, *51*, 203−220.

(3) Yang, J.; Zhang, K.-Q. Biological control of plant-parasitic nematodes by nematophagous fungi. In *Nematode-Trapping Fungi*; Zhang, K. Q., Hyde, K. D., Eds.; Vol. 23, Springer: Dordrecht, Netherlands, **2014**; pp. 231-262.

(4) Li, J., Zou, C., Xu, J., Ji, X., Niu, X., Yang, J., Huang, X., and Zhang, K.-Q. Molecular mechanisms of nematode-nematophagous microbe interactions: basis for biological control of plant-parasitic nematodes. *Annu. Rev. Phytopathol.* **2015**, *53*, 67-95.

(5) Stirling, G. R. Biological control of plant-parasitic nematodes. In *Diseases of Nematodes*; Poinar, G. O., Jansson, H.-B., Eds.; CRC Press: Boca Raton, FL, **1988**; Vol. *2*, pp 93−139.

(6) Nordbring-Hertz, B. Morphogenesis in the nematode-trapping fungus *Arthrobotrys oligospora*-an extensive plasticity of infection structures. *Mycologist.* **1999**, *18*, 125−133.

(7) Niu, X. M.; Zhang, K. Q. *Arthrobotrys oligospora*: a model organism for understanding the interaction between fungi and nematodes. *Mycology* **2011**, *2*, 59−78.

(8) Yang, J. K.; Wang, L.; Ji, X. L.; Feng, Y.; Li, X. M.; Zou, C. G.; Xu, J. P.; Ren, Y.; Mi, Q. L.; Wu, J. L. Genomic and proteomic analyses of the fungus *Arthrobotrys oligospora* provide insights into nematode-trap formation. *PLoS Pathog.* **2011**, *7*, e1002179.

(9) Stadler, M.; Sterner, O.; Anke, H. New biologically active compounds from the nematode-trapping fungus *Arthrobotrys oligospora* Fresen. *Z. Naturforsch.* **1993**, *48c*, 843–850.

(10) Anderson, M. G.; Jarman, T. B.; Rickards, R. W. Structures and absolute configurations of antibiotics of the oligosporon group from the nematode-trapping fungus *Arthrobotrys oligospora*. *J. Antibiot*. **1995**, *48*, 391–398.

(11) Wei, L. X.; Zhang, H. X.; Tan, J. L.; Chu, Y. S.; Li, N.; Xue, H. X.; Wang, Y. L.; Niu, X. M.; Zhang, Y.; Zhang, K. Q. Arthrobotrisins A-C, oligosporons from the nematode-trapping fungus *Arthrobotrys oligospora*. *J. Nat. Prod.* **2011**, *74*, 1526–1530.

(12) Zhang, H. X.; Tan, J. L.; Wei, L. X.; Wang, Y. L.; Zhang, C. P.; Wu, D. K.; Zhu, C. Y.; Zhang, Y.; Zhang, K. Q.; Niu, X. M. Morphology regulatory metabolites from *Arthrobotrys oligospora*. *J. Nat. Prod.* **2012**, *75*, 1419–1423.

(13) Huffman, J.; Gerber, R.; Du, L. Recent advancements in the biosynthetic mechanisms for polyketide-derived mycotoxins. *Biopolymers*. **2010**, *93*, 764–776.

(14) Tannous, J.; El Khoury, R.; Snini, S. P.; Lippi, Y.; El Khoury, A.; Atoui, A.; Lteif, R.; Oswald, I. P.; Puel, O. Sequencing, physical organization and kinetic expression of the patulin biosynthetic gene cluster from *Penicillium expansum*. *Int. J. Food Microbiol*. **2014**, *189*, 51–60.

(15) Xu, Z. F.; Wang, B. L.; Sun, H. K.; Yan, N.; Zeng, Z. J.; Zhang, K. Q.; Niu, X. M. High trap formation and low metabolite production by disruption of the polyketide synthase gene involved in the biosynthesis of arthrosporols from nematode-trapping fungus *Arthrobotrys oligospora*. *J. Agric. Food Chem.* **2015**, *63*, 9076–9082.

(16) Xu, Z. F.; Chen, Y. H.; Song, T. Y.; Zeng, Z. J., Yan, N.; Zhang, K. Q.; Niu, X. M. Nematicidal key precursors for the biosynthesis of morphological regulatory arthrosporols in the nematode-trapping fungus *Arthrobotrys oligospora*. *J. Agric. Food Chem.* **2016**, *64*, 7949–7956.

(17) Weber, T.; Blin, K.; Duddela, S.; Krug, D.; Kim, H. U.; Bruccoleri, R.; Lee, S. Y.; Fischbach, M. A.; Müller, R.; Wohlleben, W.; Breitling, R.; Takano, E.; Medema, M. H. antiSMASH 3.0-A comprehensive resource for the genome mining of biosynthetic gene clusters. *Nucleic Acids Res*. **2015**, *43*, W237−W243.

(18) Mitchell, A,; Chang, H.; Daugherty, L.; Fraser, M.; Hunter, S.; Lopez, R.; McAnulla, C.; McMenamin, C.; Nuka, G.; Pesseat, S.; Sangrador-Vegas, A.; Scheremetjew, M.; Rato, C.; Yong, S.; Bateman, A.; Punta, M.; Attwood, T. K.; Sigrist, C. J.A.; Redaschi, N.; Rivoire, C.; Xenarios, I.; Kahn, D.; Guyot, D.; Bork, P.; Letunic, I.; Gough, J.; Oates, M.; Haft, D.; Huang, H.; Natale, D. A.; Wu, C. H.;

Orengo, C.; Sillitoe, I.; Mi, H.; Thomas, P. D.; Finn, R. D. The InterPro protein families database: the classification resource after 15 years. *Nucleic Acids Res.,* **2015**, doi: 10.1093/nar/gku1243.

(19) Benson, D. A.; Cavanaugh, M.; Clark K, K. I.; Lipman D. J. GenBank. *Nucleic Acids Res*. **2013**, *41(D1)*, D36–42.

(20) Zhao, X. Y.; Wang, Y. C.; Zhao, Y.; Huang, Y.; Zhang, K. Q.; Yang, J. K. Malate synthase gene AoMls in the nematode-trapping fungus *Arthrobotrys oligospora* contributes to conidiation, trap formation, and pathogenicity. *Appl. Microbiol. Biotechnol.* **2014**, *98*, 2555–2563.

(21) Molyneux, R. J.; Schieberle, P. Compound identification: a journal of agricultural and food chemistry perspective. *J. Agric. Food Chem.* **2007**, 55, 4625–4629.

(22) Holm, D. K.; Petersen, L. M.; Klitgaard, A.; Knudsen, P. B.; Jarczynska, Z. D.; Nielsen, K. F.; Gotfredsen, C. H.; Larsen, T. O.; Mortensen, U. H. Molecular and chemical characterization of the biosynthesis of the 6-MSA-Derived meroterpenoid yanuthone d in *Aspergillus niger*. *Chem. Biol.* **2014**, *21*, 519–529.

(23) Bugni, T. S.; Abbanat, D.; Bernan, V. S.; Maiese, W. M.; Greenstein, M.; Van Wagoner, R. M.; Ireland, C. M. Yanuthones: novel metabolites from a marine isolate of *Aspergillus niger*. *J. Org. Chem.* **2000**, *65*, 7195-7200.

(24) Mehta, G.; Pan, S. C. First total synthesis of yanuthones: novel farnesylated epoxycyclohexenoid marine natural products. *Tetrahedron lett.* **2005**, *46*, 5219-5223.

(25) Petersen, L. M.; Holm, D. K.; Knudsen, P. B.; Nielsen, K. F.; Gotfredsen, C. H.; Mortensen, U. H.; Larsen, T. O. Characterization of four new antifungal yanuthones from *Aspergillus niger*. *J. Antibiot.* **2015**, *68,* 201-205.

401

402 Table 1. Primers used for construction of the knockout vector of the gene *AOL_s00215g280*. M:

403 mutant Δ *AOL_s00215g280*; WT: wildtype strain.

Name	*Insertion sites in pAg1-H3*	Sequence 5'→3'	Fragment Size
280L-5f	*Sma1*	GAGCTCGGTACCAAGGCCCGGGGTTAGGACCGT CGATGAC	2064
280L-3r	*Apa1*	AGGCCTGATCATCGATGGGCCCAACCCAAAGCTC AATCTGTA	
280R-5f	*Fse1*	ACTAGTGCGCGATCGCGGCCGGCCTTTTGTGGAG GACTGGGTC	1812
280R-3r	*Pac1*	ATGCCTGCAGGTCGACATTAATTAAATCGGGTGA ACAGCGTAA	
280yz-5f		GGGAACAAGTCTGGGTTAA	2976 (M) 1317 (WT)
280yz-3r		TGCACGGAGTTCATGGTA	

404

405

406 Table 2. The 1D and 2D NMR spectroscopic data of **$C_{280\text{-}1}$-$C_{280\text{-}3}$**.

	$C_{280\text{-}1}$[a]		**$C_{280\text{-}2}$**[b]		**$C_{280\text{-}3}$**[b]	
No	δ_H (multi, *J* in Hz)	δ_C	δ_H (multi, *J* in Hz)	δ_C	δ_H (multi, *J* in Hz)	δ_C
1	4.24, s	67.4, CH	4.39, s	67.2, CH	4.38, s	67.1, CH
2		158.0, C		157.1, C		157.1, C
2-CH_3	1.91, s	21.2, CH_3	2.00, s	21.2, CH_3	2.00, s	21.3, CH_3
3	5.68, s	124.7, CH	5.74, s	124.5, CH	5.74, s	124.3, CH
4		195.6, C		194.3, C		194.2, C
5		60.2, C		59.6, C		59.4, C
6	3.53, s	63.9, CH	3.63, s	62.5, CH	3.63, s	62.1, CH
1'	2.10, overlap	28.3, CH_2	2.73, m	27.2, CH_2	2.31, dd (12, 6)	27.7, CH_2
			2.42, m		2.16, t (12.5)	
2'	2.03, overlap	35.5, CH_2	5.09, t (14.1)	118.4, CH	5.12, t (11.5)	118.9, CH
3'		138.8, C		139.5, C		138.8, C
3'-CH_3	1.56, s	16.3, CH_3	1.12, d (7.2)	17.7, CH_3	1.67, s	16.3, CH_3
4'	5.24, t (11.5)	118.5, CH	2.00, m	40.4, CH_2	2.31, dd (12, 6)	39.2, CH_2
					2.16, t (12.5)	
5'	2.90, d (5.5)	34.7, CH_2	1.60, overlap	26.3, CH_2	2.71, m	26.9, CH_2
			1.44, overlap		2.46, m	
6'		177.2, C	1.60, overlap	34.1, CH_2	6.74, t (11.5)	142.5, CH
			1.44, overlap			
7'			2.42, m	39.8, CH		128.9, C
			1.12, d (7.1)			
7'-CH_3			1.63, s	16.4, CH_3	1.80, s	12.7, CH_3
8'				177.9, C		169.5, C

[a]Recorded in CD_3OD. [b]Recorded in acetone-d_6.

407

408

409

410 **Figure Captions**

411 **Figure 1.** The representative structures of the PKS-TPS hybrid metabolites (**1-7**) and their precursors
412 (**9**-**10**) isolated from nematode-trapping fungus *A. oligospora*, and isoepoxydon (**8**).

413

414 **Figure 2.** Phylogenetic analysis based on the deduced amino acid sequence of AOL_s00215g280 and
415 other related proteins from different fungi. The amino acid sequences of these proteins were aligned
416 with Clustal X version 1.83, and MEGA 5.04 was used to construct a neighbor-joining tree, including
417 bootstrap analysis with 1,000 replicates. Numbers below nodes indicate the bootstrap value. The bar
418 marker indicates the genetic distance, which is proportional to the number of amino acid substitutions.
419 GenBank accession numbers are given in brackets.

420

421 **Figure 3.** (A) The gene cluster *AOL_s00215* containing twelve genes and spanning 51.843 kb;
422 *AOL_s00215g280* (putatively encoding cytochrome P450), *AOL_s00215g281* (encoding decarboxylase
423 for 6-methylsalicylic acid synthase), *AOL_s00215g282* (encoding cytochrome P450 for *m*-cresol), and
424 *AOL_s00215g283* (encoding 6-methylsalicylic acid synthase); (B) The sketch map of replacement of
425 targeting gene *AOL_s00215g280* using homologous recombination method. (C) Transformants of
426 Δ*AOL_s00215g280* were screened out and confirmed by PCR method; W: the wildtype strain as
427 negative control; M, marker (DL5000); lanes 1-23: transformants; lanes 1, 2 and 10, three mutants with
428 the total knockout of the gene Δ*AOL_s00215g280*.

429

430 **Figure 4.** Comparison of the growth of the wildtype and the mutant Δ*AOL_s00215g280* strains on
431 PDA, TYGA or YMA, for 4, 6, 8, and 10 d at 28°C. WT: wildtype strain; 280: Δ*AOL_s00215g280*.

432

433 **Figure 5.** (A) Comparison of the conidial formation between the wildtype strain and the mutant
434 Δ*AOL_s00215g280*. (B) Comparison of the spore germination rates between the wildtype strain and the
435 mutant Δ*AOL_s00215g280*. (C) Comparison of the trap formation of the wildtype strain and the mutant

436 Δ*AOL_s00215g280*, red arrow: traps around the bodies of nematodes. (D) Comparison of the captured
437 nematodes of the wildtype strain and the mutant Δ*AOL_s00215g280*. WT: the wildtype strain; 280: the
438 mutant Δ*AOL_s00215g280*; **P*<0.05 versus wildtype strain; ***P*<0.01 versus wildtype strain;
439 ****P*<0.001 versus wildtype strain.
440
441 **Figure 6.** HPLC analysis of the methanol extracts of the cultural broths from the wildtype strain (black
442 line) and the mutant Δ*AOL_s00215g280* (red line), and of the standard sample arthrosporol A.
443
444 **Figure 7.** The new intermediate metabolites (**11-13**) from the mutant Δ*AOL_s00215g280* of nematode-
445 trapping fungus *A. oligospora*, and the key HMBC, $^{1}H-^{1}H$ COSY, and NOESY correlations of **11**
446 (indicated by arrows).
447
448 **Figure 8.** The inhibitory effects of the three intermediate metabolites $\mathbf{C_{280\text{-}1}}$-$\mathbf{C_{280\text{-}3}}$ (**11-13**) from the
449 mutant Δ*AOL_s00215g280* of nematode-trapping fungus *A. oligospora*. **A**: avermectins.
450
451
452
453

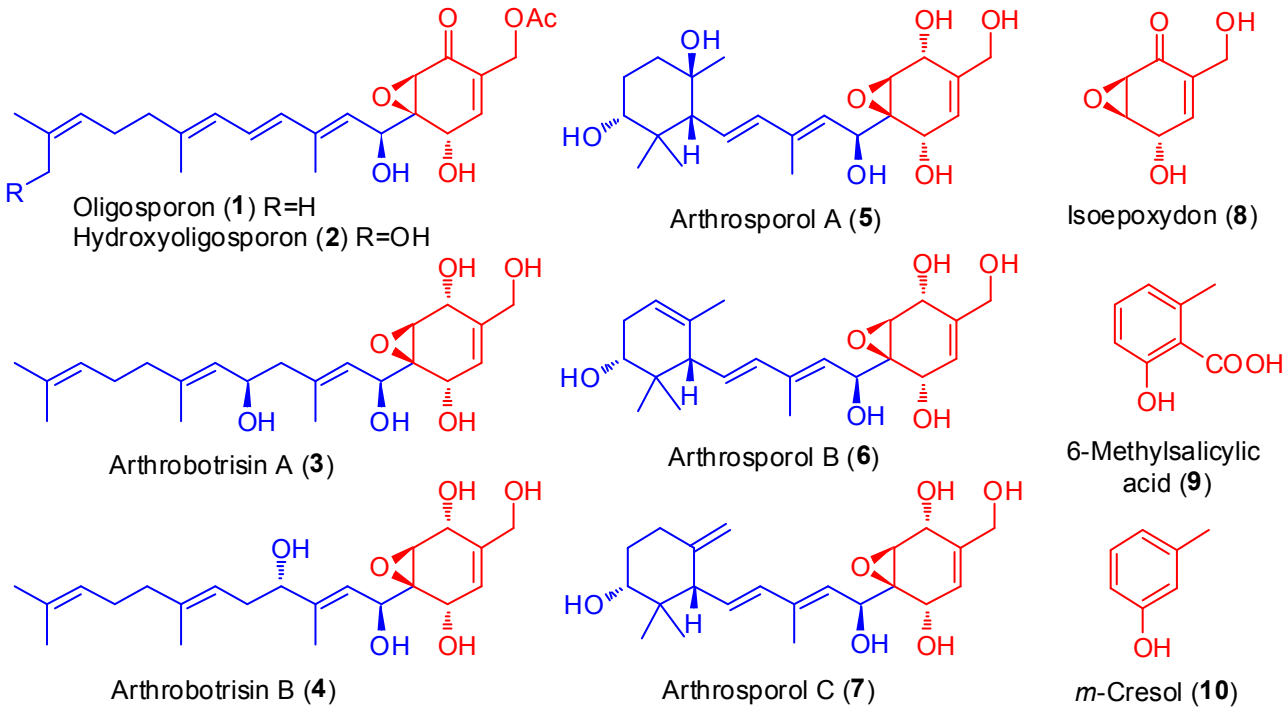

454

455 **Figure 1.**

456

457

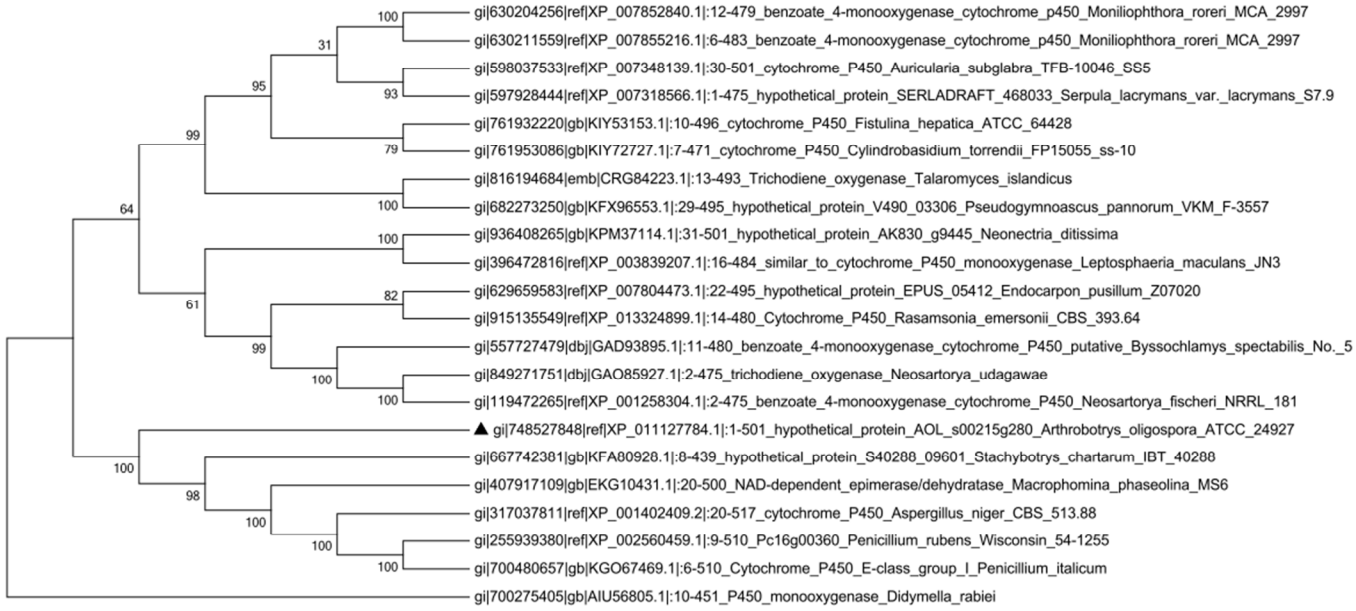

458

459 **Figure 2.**

460

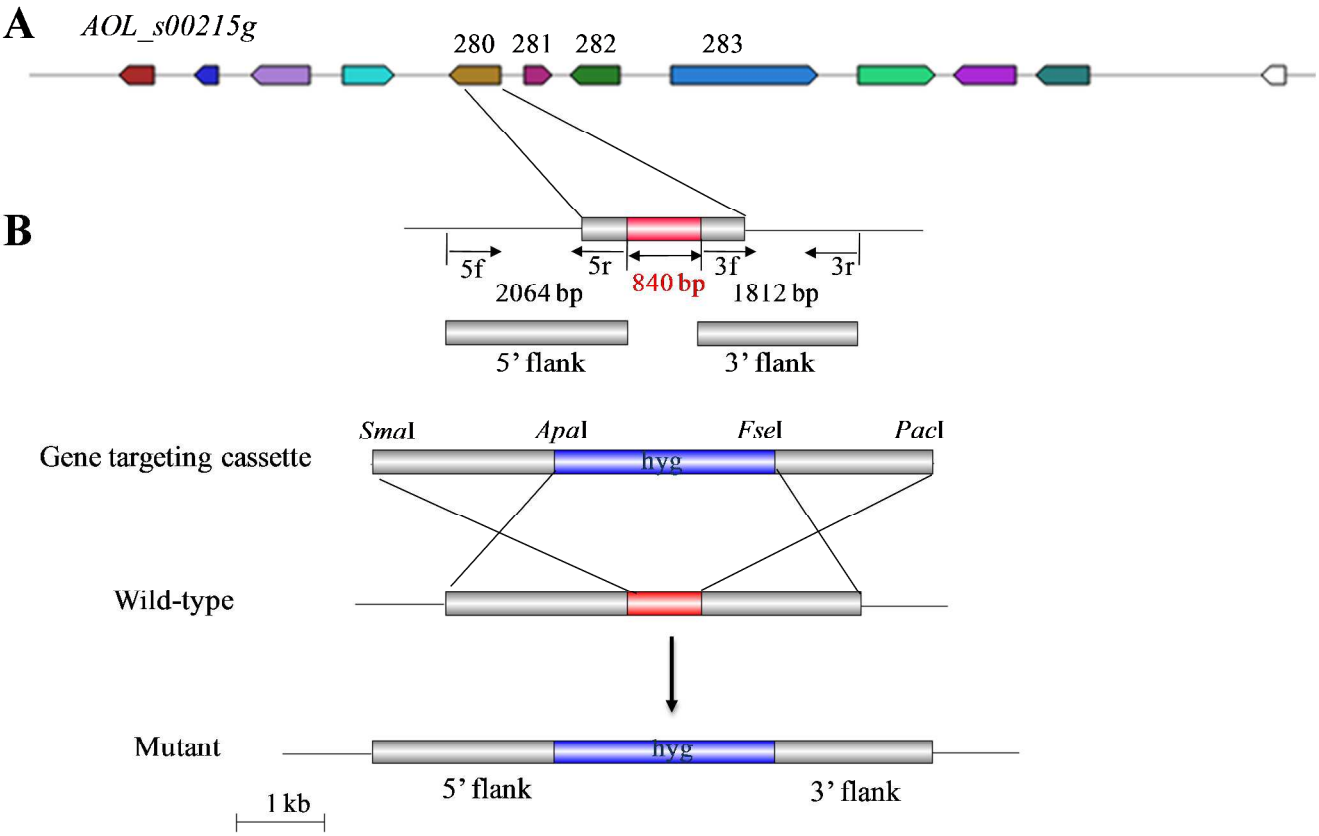
A
AOL_s00215g
280 281 282 283
B
5f
5r
840 bp
3f
3r
2064 bp
1812 bp
5' flank
3' flank
Gene targeting cassette
SmaI
ApaI
FseI
PacI
hyg
Wild-type
Mutant
hyg
5' flank
3' flank
1 kb

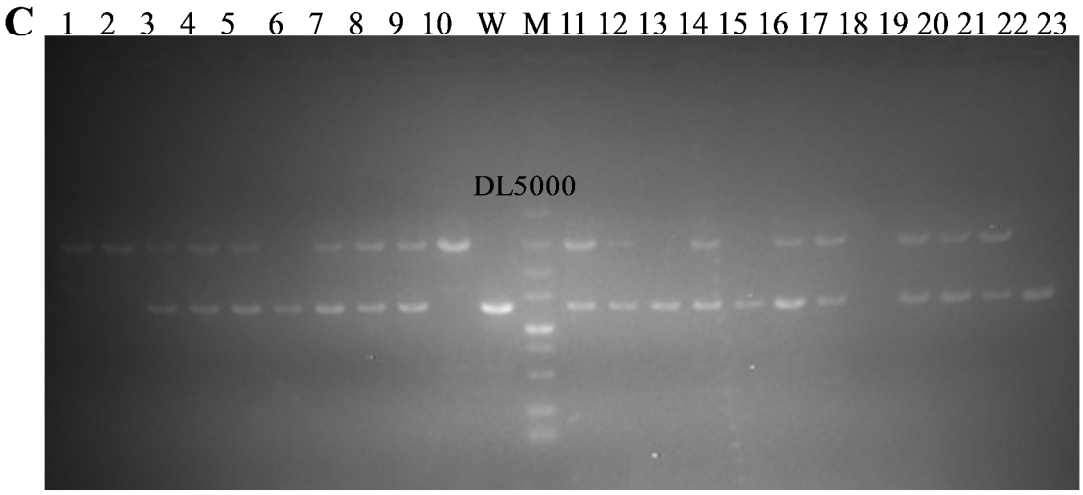
C
1 2 3 4 5 6 7 8 9 10 W M 11 12 13 14 15 16 17 18 19 20 21 22 23
DL5000

Figure 3.

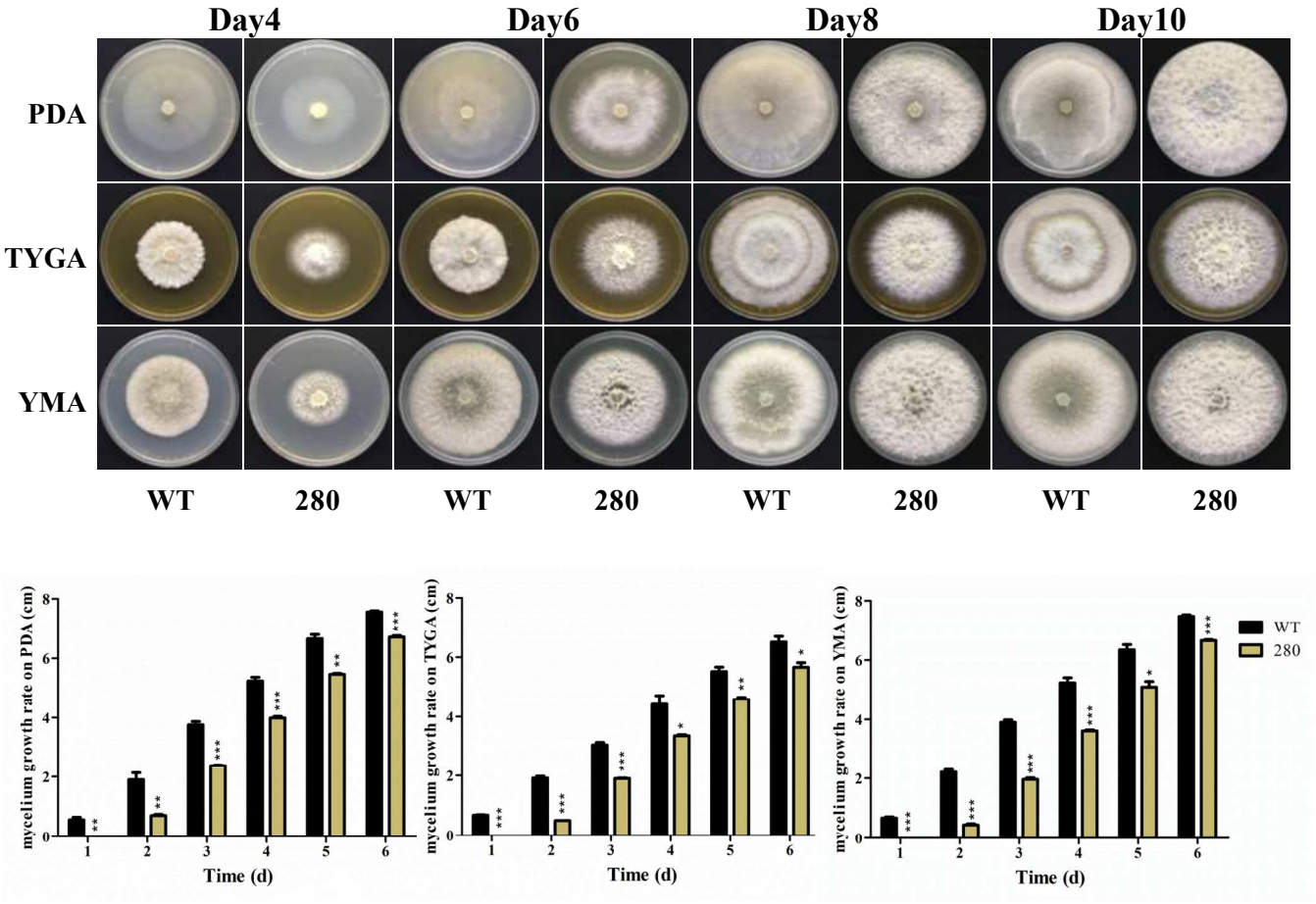
Day4
Day6
Day8
Day10
PDA
TYGA
YMA
WT
280
WT
280
WT
280
WT
280
mycelium growth rate on PDA (cm)
mycelium growth rate on TYGA (cm)
mycelium growth rate on YMA (cm)
Time (d)
Time (d)
Time (d)
WT
280

Figure 4.

469

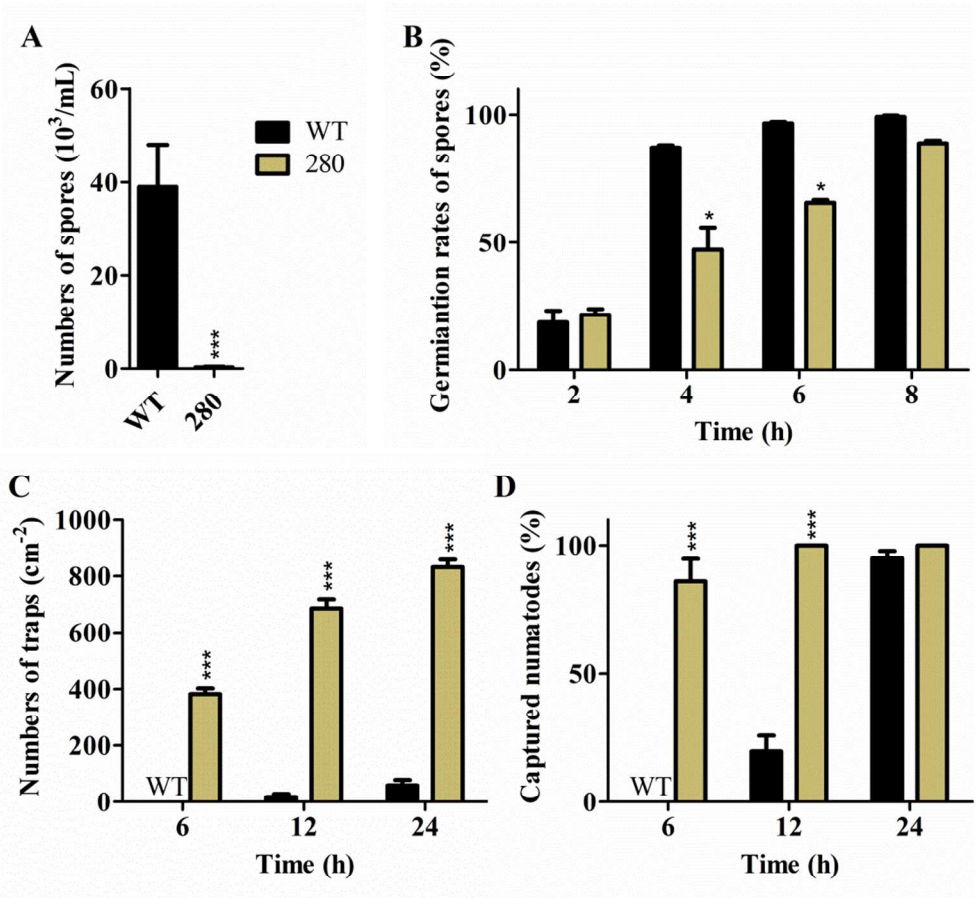

470

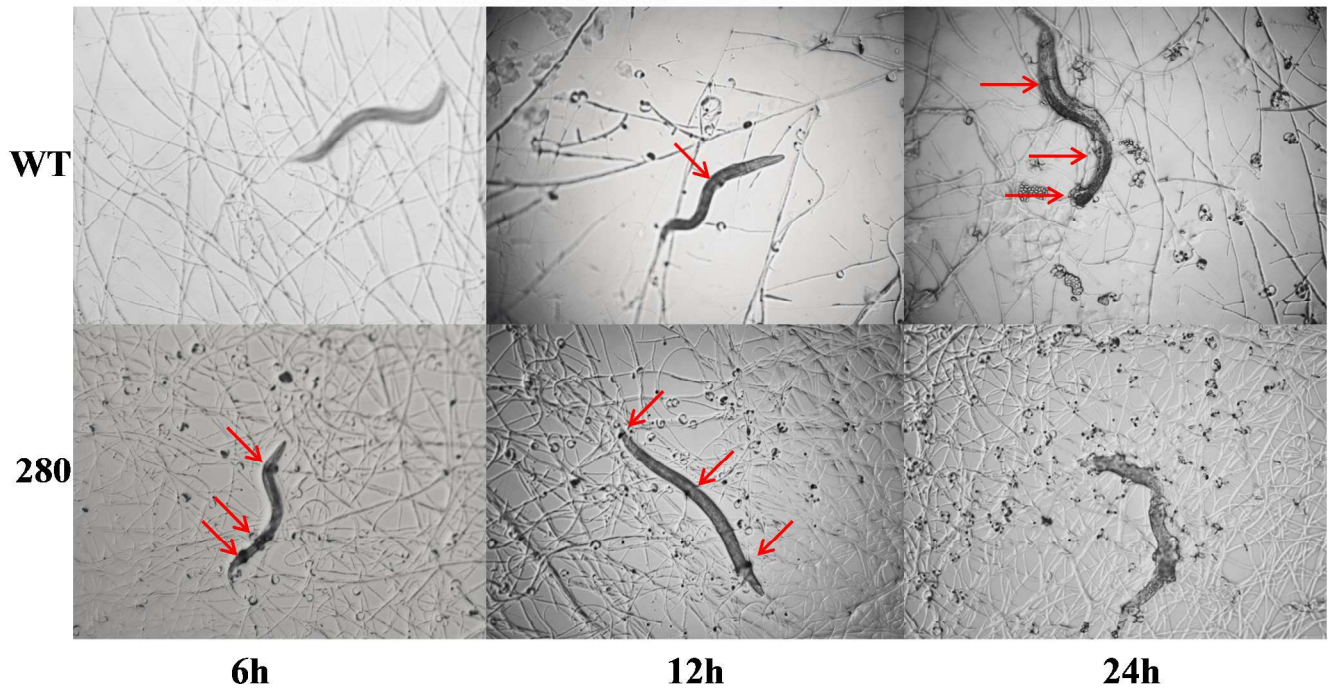

471

472 **Figure 5.**

473

474

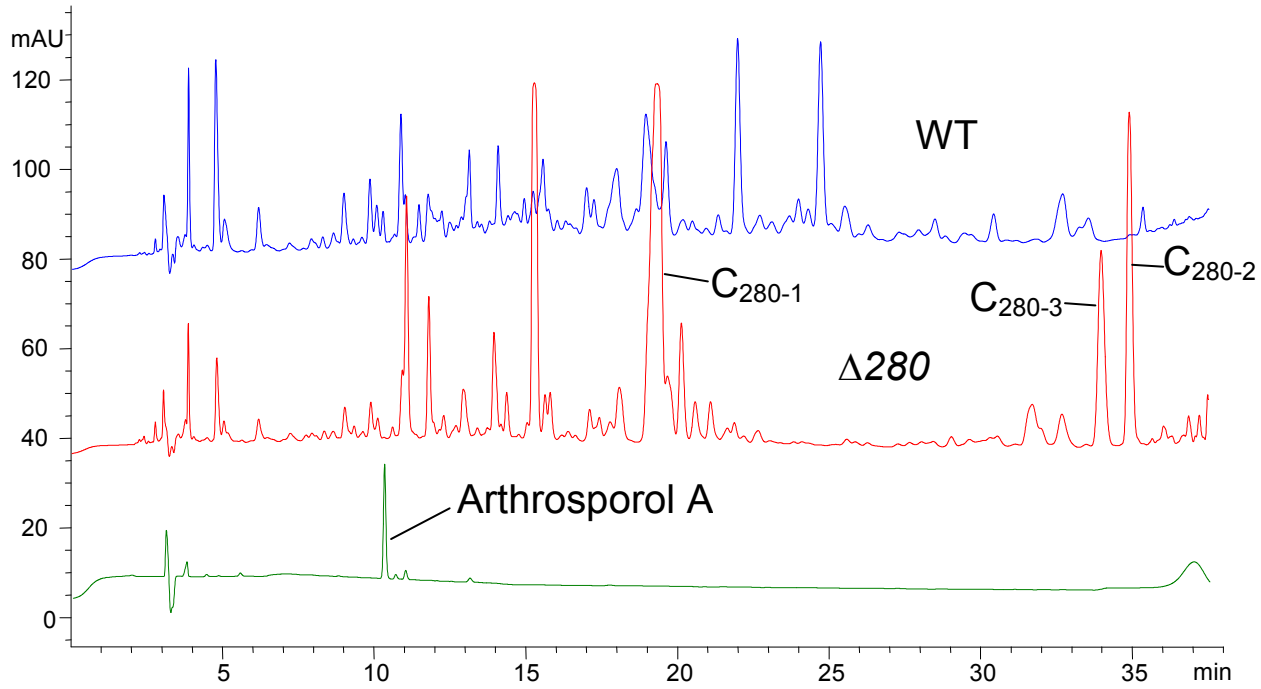

475

476 **Figure 6.**

477

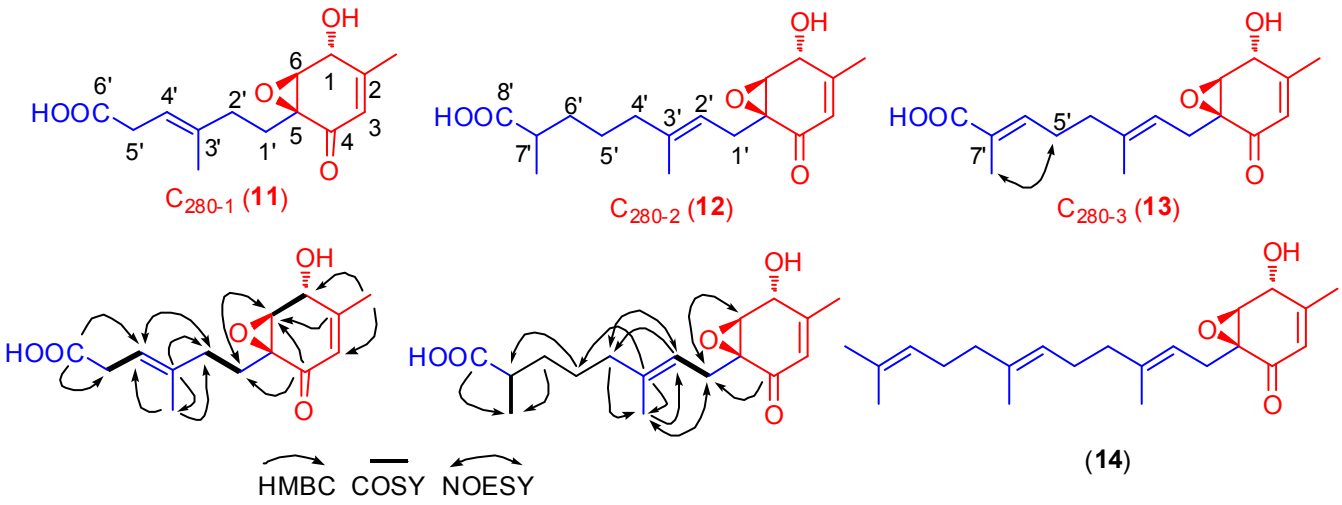

Figure 7.

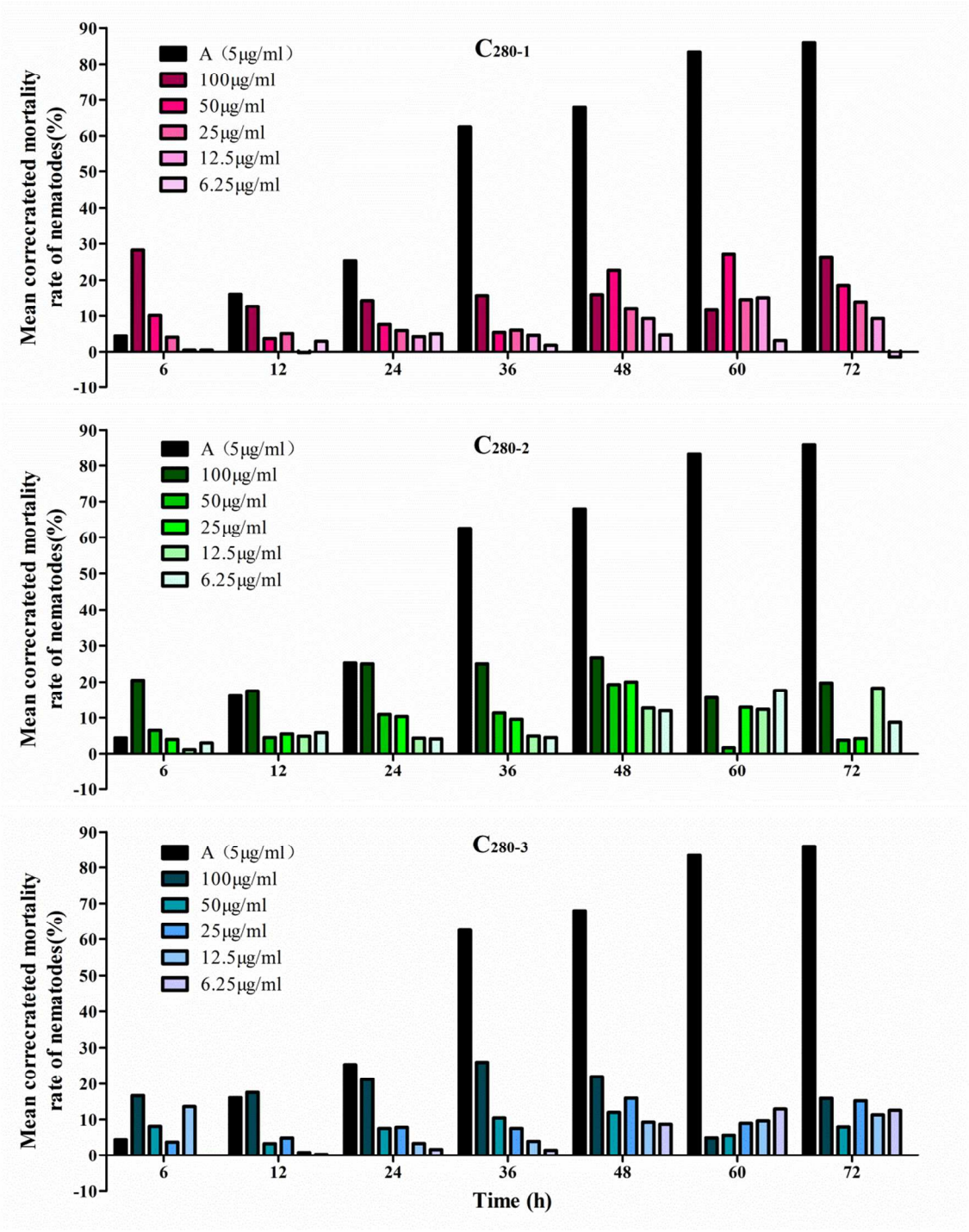
C280-1
A（5μg/ml）
100μg/ml
50μg/ml
25μg/ml
12.5μg/ml
6.25μg/ml
Mean correcrateted mortality rate of nematodes(%)
C280-2
C280-3
Time (h)

Figure 8.

489 **Table of Contents Graphic**

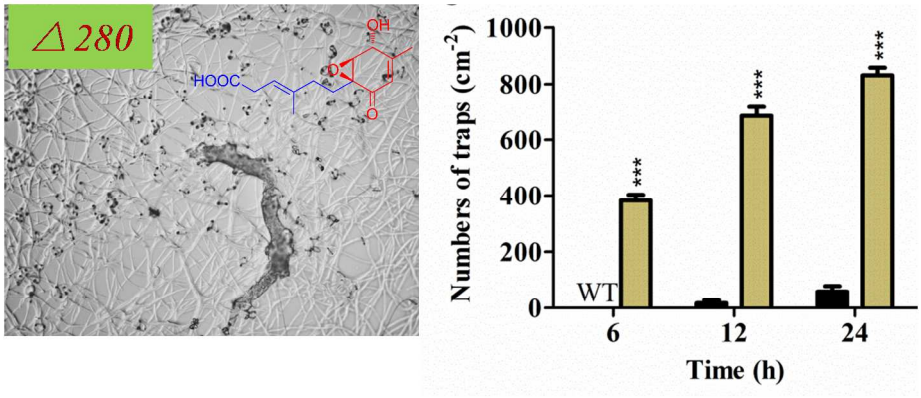

490

491